

Supplementary Information

Why do Some Metal Ions Spontaneously Form Nanoparticles in Water Microdroplets: Disentangling the Contributions of the Air–Water Interface and Bulk Redox Chemistry

Muzzamil Ahmad Eatoo^{a,b,c,d}, Nimer Wehbe^e, Najeh Kharbatia^b, Xianrong Guo^e, Himanshu
Mishra^{a,b,c,d*}

^aEnvironmental Science and Engineering (EnSE) Program, Biological and Environmental
Science and Engineering (BESE) Division, King Abdullah University of Science and
Technology (KAUST), Thuwal, 23955-6900, Kingdom of Saudi Arabia

^bWater Desalination and Reuse Center (WDRC),
King Abdullah University of Science and Technology (KAUST), Thuwal, 23955-6900,
Kingdom of Saudi Arabia

^cCenter for Desert Agriculture (CDA), King Abdullah University of Science and Technology
(KAUST), Thuwal 23955-6900, Saudi Arabia

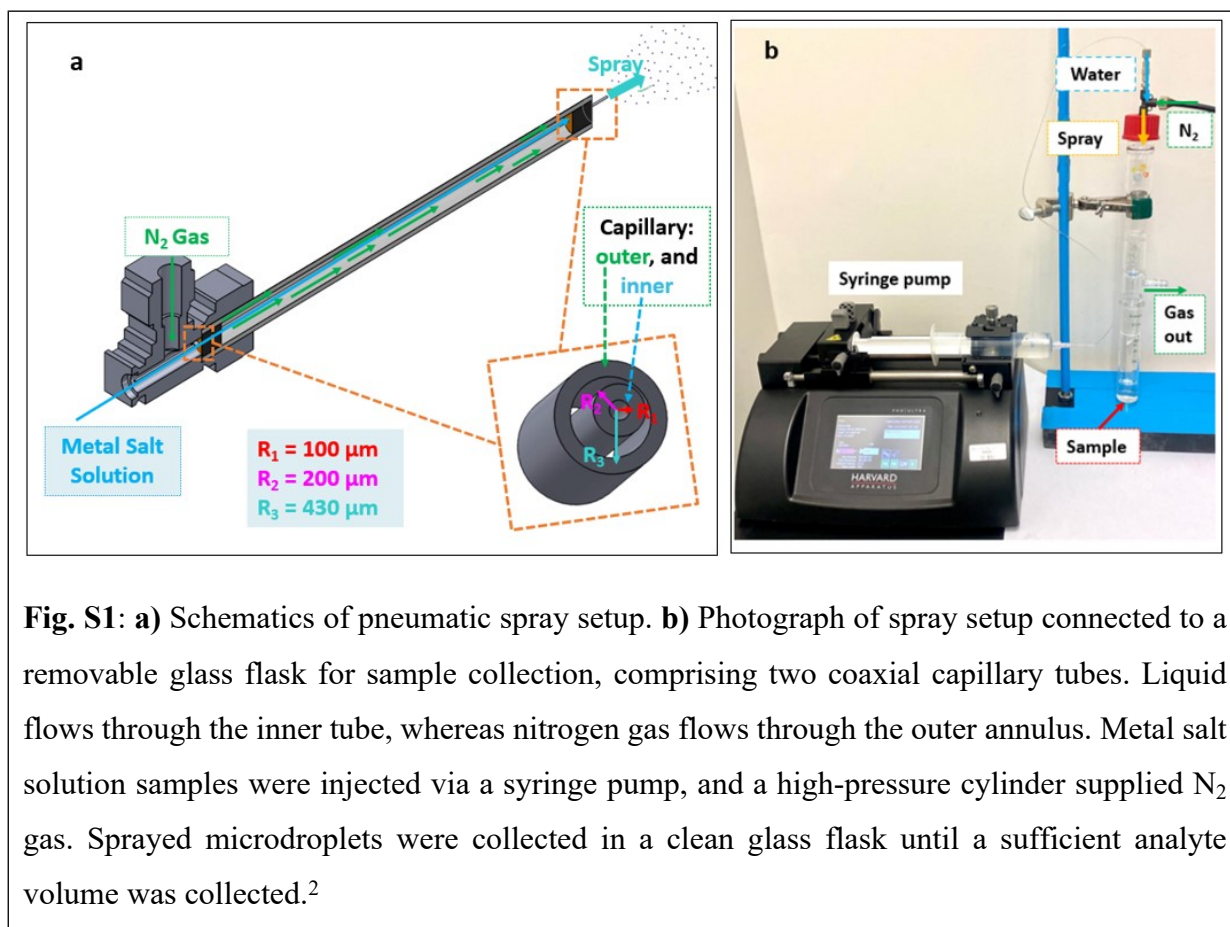
^dInterfacial Lab (iLab), King Abdullah University of Science and Technology (KAUST),
Thuwal 23955-6900, Saudi Arabia

^eCore Labs, King Abdullah University of Science and Technology (KAUST), Thuwal 23955-
6900, Saudi Arabia

*Correspondence: himanshu.mishra@kaust.edu.sa

Section S1: Water microdroplet generation via sprays

We adapted the experimental setup built by Gallo et al.¹ to produce water microdroplets. In a coaxial system, water was injected through an inner tube with a 100- μm diameter using a syringe pump (PHD Ultra, Harvard Apparatus). Dry $\text{N}_2(\text{g})$ was pushed through the outer tube with a 430- μm diameter. Additionally, HPLC-grade water was used to make salt solutions, and a glass cell (equipped with a tiny opening to prevent pressure build-up) was employed to collect microdroplets while minimizing ambient contamination. The water flow rate was 25 $\mu\text{L}/\text{min}$, whereas the gas (N_2) pressure was 100 psi.



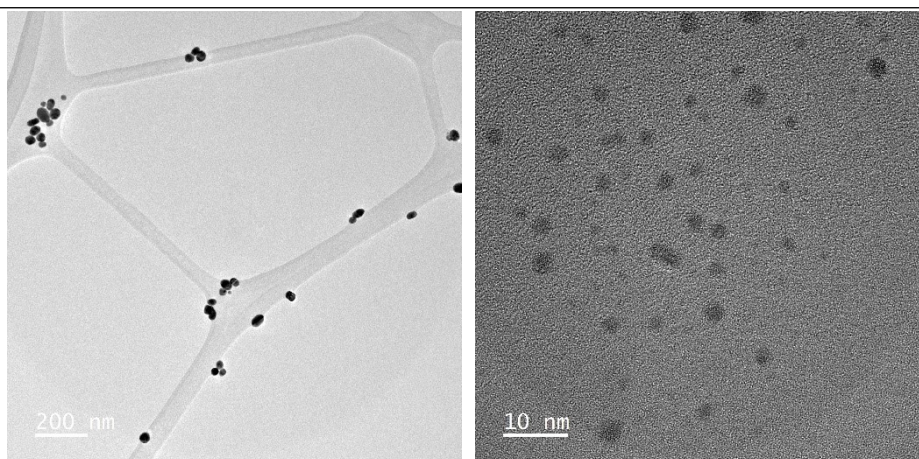


Fig. S2 TEM imaging of microdroplets samples formed by spraying 100 μM HAuCl_4 solution, collected and drop cast, shows the presence of AuNPs.

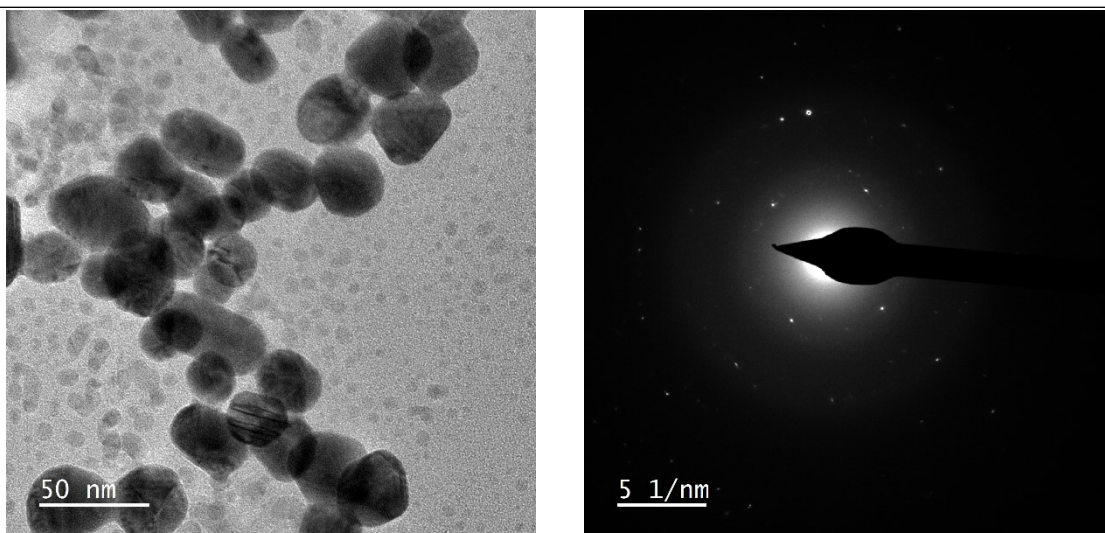


Fig. S3 TEM imaging of bulk aqueous 100 μM HAuCl_4 solution: Micrograph showing the presence of nanoparticles of different sizes and diffraction pattern showing the formation of $\text{Au}(0)$.

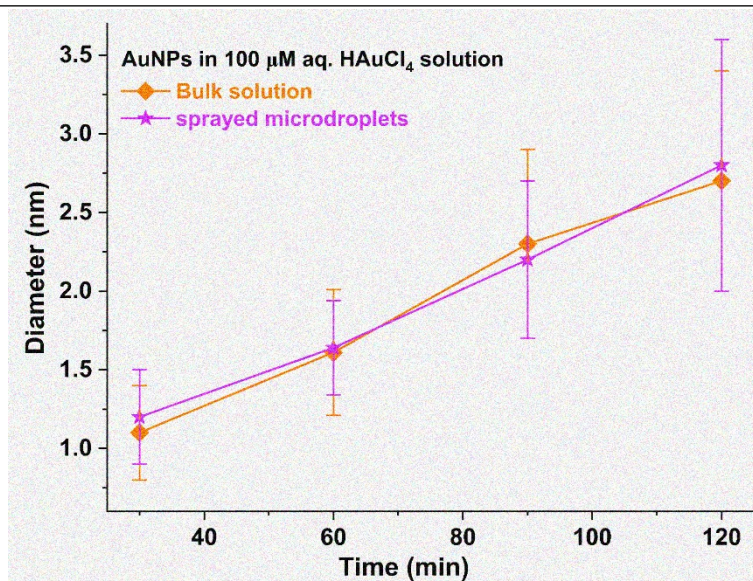


Fig. S4 DLS measurements of the sizes of nanoparticles formed in bulk solutions and sprays. Typical sample's age, i.e., the time on the x-axis, depends on sample preparation (~ 5 mins), the water flow rate during spraying (viz., 25, 50, 75, and 100 $\mu\text{L}/\text{min}$), and subsequent DLS measurements. Since the particles size distributions are indistinguishable between bulk solutions and sprays, the effects of microdroplet geometry or the air–water interface seem to be negligible on NP formation.

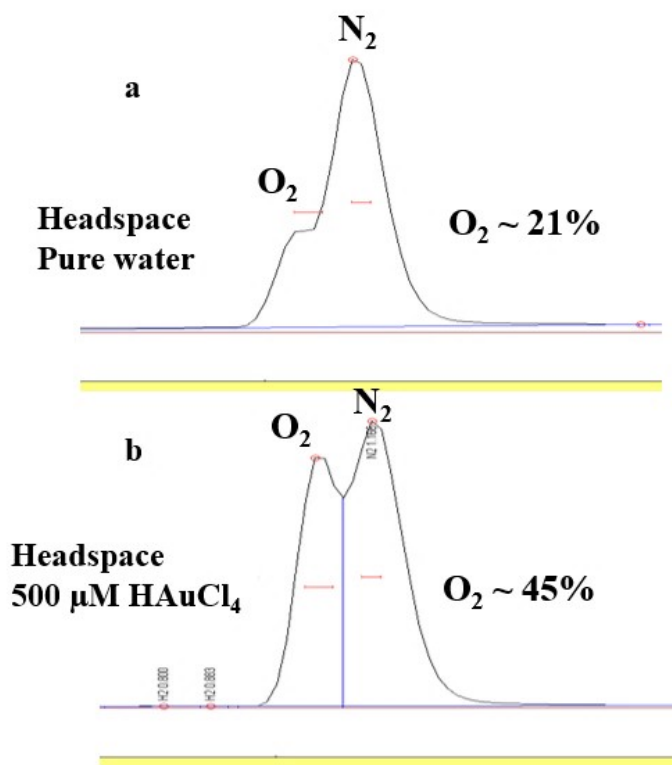
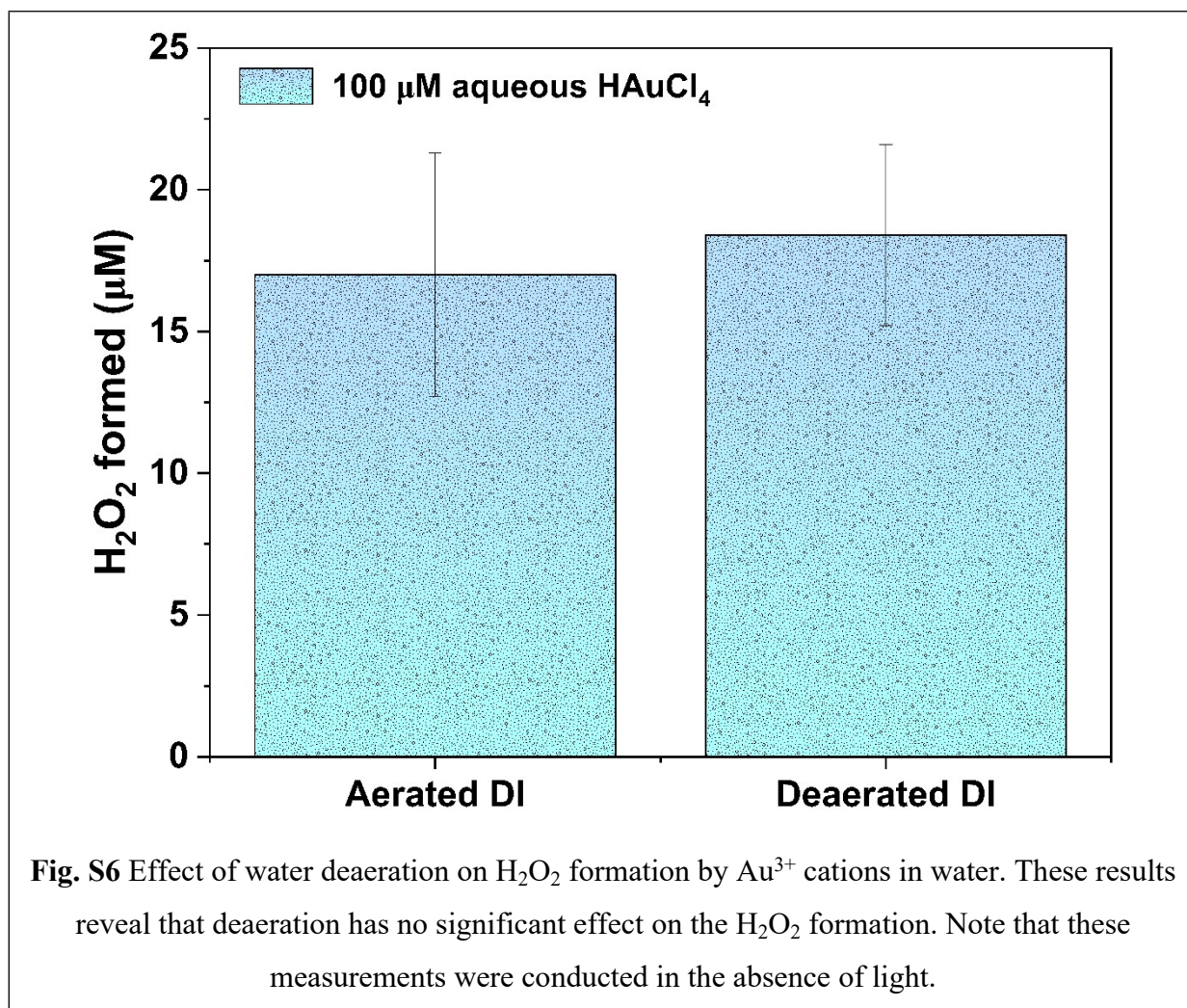
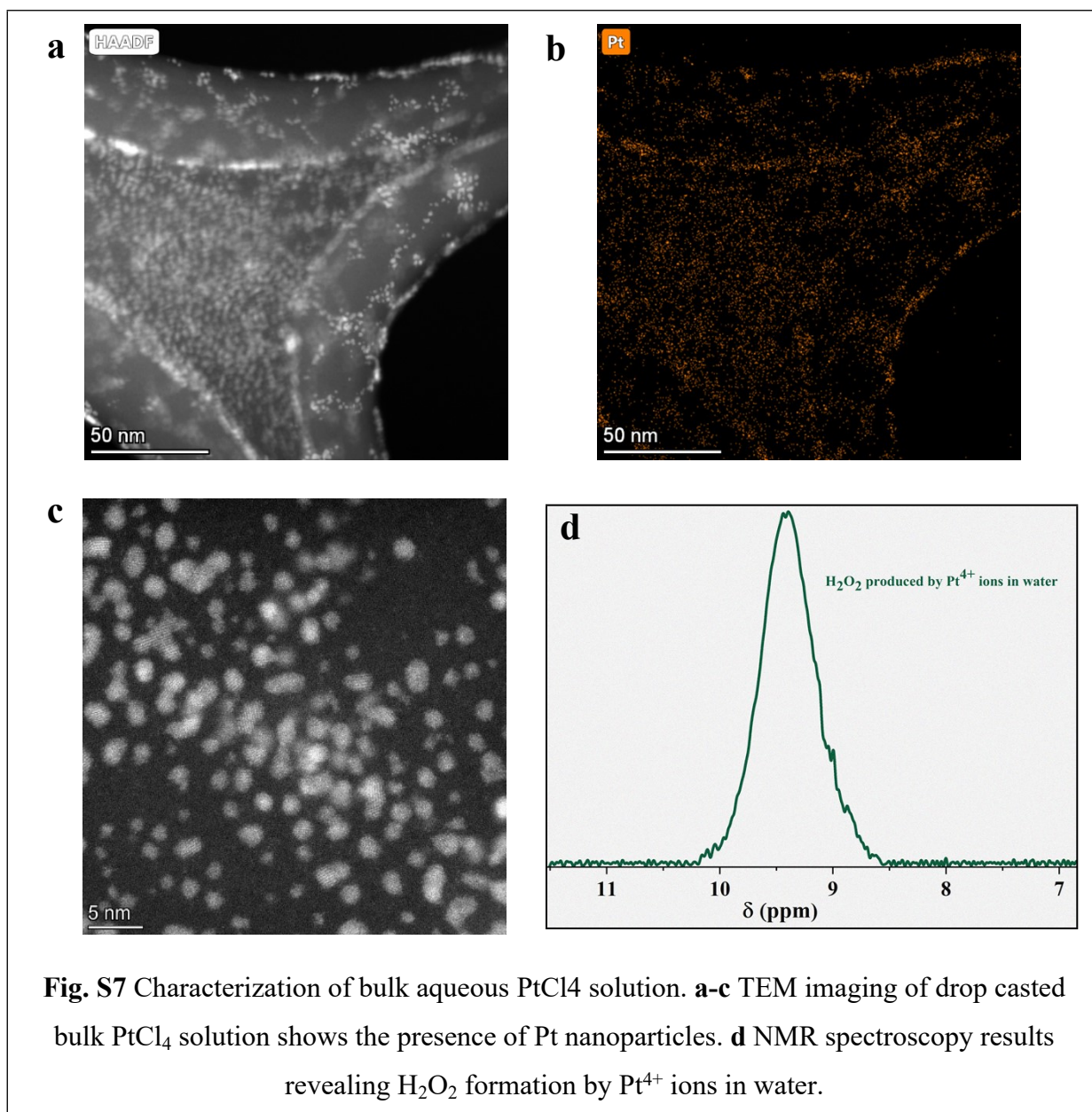


Fig. S5: Gas chromatography results show oxygen gas evolution from the HAuCl₄ aqueous solution. **a** showing the presence of around 21% oxygen in the headspace of pure water (DI used for making solutions). **b** shows the presence of around 45% oxygen in the headspace of 500 μM HAuCl₄ solution after the age of around 24 h. This reveals that the HAuCl₄ solution evolves oxygen gas.



In order to investigate whether the presence of H_2O_2 in the gold salt solutions resulted from an oxygen reduction reaction or light exposure, the measurements were carried out under conditions where dissolved oxygen was removed from the water and in the absence of light. The findings indicated that the H_2O_2 present in the gold salt solution did not originate from an oxygen reduction reaction, nor was it induced by light.



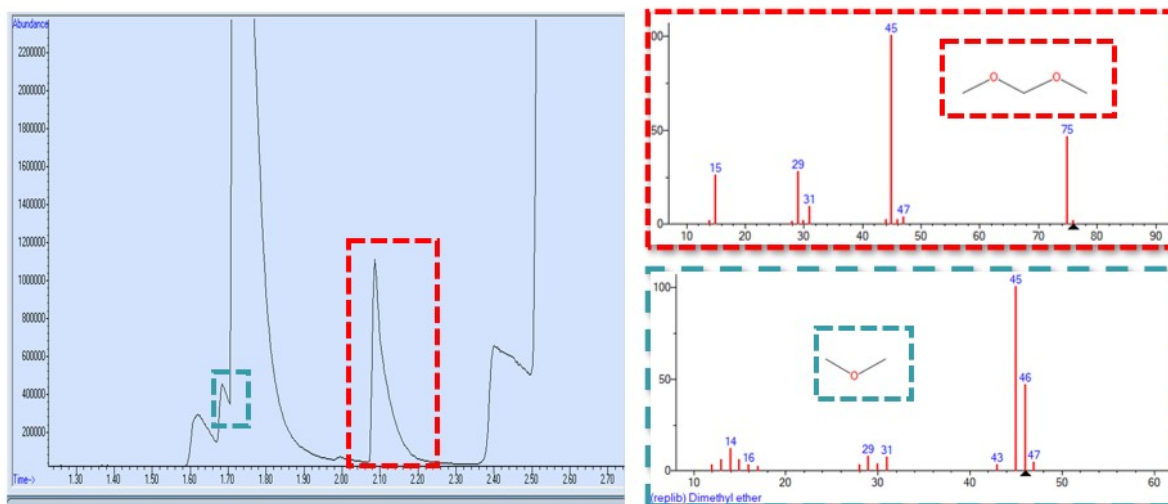


Fig. S8 GC-MS for H_{AuCl₄} salt in methanol. The results reveal the presence of Methylal (CH₃OCH₂OCH₃) and Dimethyl ether (CH₃OCH₃)

Table S1 Summary of some key observations in this study

Solvent	Environment (bulk or microdroplet)	Formation of Nanoparticles $M^{n+} + ne^- = M$ (s)	Metal ions which form H_2O_2	Kinetics of Formation of Nanoparticles $M^{n+} + ne^- = M$ (s)
Water	Bulk	Au and Pt nanoparticles	Au^{3+} , Pt^{4+} , Fe^{3+}	Fast
	Microdroplet			
Methanol	Bulk	Au and Pt nanoparticles	Au^{3+} , Pt^{4+} , Fe^{3+}	Fast
Ethanol	Bulk	Au and Pt nanoparticles	Au^{3+} , Pt^{4+} , Fe^{3+}	Fast
Acetonitrile	Bulk	Negligible NPs formation	No H_2O_2	Sluggish

Table S2:

Standard electrochemical series with the standard reduction potentials:

Standard Reduction Half-Reaction	Standard Reduction Potential E° (volts)
$\text{Au}^+ + e^- \rightleftharpoons \text{Au}(s)$	1.83
$\text{Au}^{3+} + 3e^- \rightleftharpoons \text{Au}(s)$	1.52
$\text{Au}^{3+} + 2e^- \rightleftharpoons \text{Au}^+$	1.36
$\text{AuCl}_4^- + 3e^- \rightleftharpoons \text{Au}(s) + 4\text{Cl}^-$	1.002
$\text{AuCl}_4^- + 2e^- \rightleftharpoons \text{AuCl}_2^- + 2\text{Cl}^-$	0.926
$\text{Pt}^{2+} + 2e^- \rightleftharpoons \text{Pt}(s)$	1.2
$\text{PtCl}_2 + 2e^- \rightleftharpoons \text{Pt}(s) + 4\text{Cl}^-$	0.78
$\text{PtCl}_4 + 2e^- \rightleftharpoons \text{PtCl}_2 + 2\text{Cl}^-$	0.75
$\text{Fe}^{3+} + e^- \rightleftharpoons \text{Fe}^{2+}$	0.771
$\text{H}_2\text{O}_2 + \text{H}^+ + e^- \rightleftharpoons \text{HO}^* + \text{H}_2\text{O}$	0.710
$\text{O}_2(\text{g}) + 2\text{H}^+ + 2e^- \rightleftharpoons \text{H}_2\text{O}_2$	0.695
$\text{O}_2(\text{g}) + 2\text{H}_2\text{O}(\text{l}) + 4e^- \rightleftharpoons 4\text{OH}^-$	0.401
$\text{Cu}^{2+} + 2e^- \rightleftharpoons \text{Cu}$	0.34
$\text{Fe}^{3+} + 3e^- \rightleftharpoons \text{Fe}(s)$	-0.037
$\text{Ti}^{2+} + 2e^- \rightleftharpoons \text{Ti}(s)$	-0.163
$\text{Ti}^{3+} + e^- \rightleftharpoons \text{Ti}^{2+}$	-0.37
$\text{Fe}^{2+} + 2e^- \rightleftharpoons \text{Fe}(s)$	-0.44
$\text{Zn}^{2+}(\text{aq}) + 2e^- \rightleftharpoons \text{Zn}(s)$	-0.76
$\text{Al}^{3+} + 3e^- \rightleftharpoons \text{Al}(s)$	-1.706
$\text{Mg}^{2+} + 2e^- \rightleftharpoons \text{Mg}(s)$	-2.356

Section S2: Confirmation of H₂O₂ peak position

To confirm that the obtained peak positioned at a chemical shift around 9.4 ppm in gold ion solution (0.3M H_{AuCl₄} in water) corresponds to the H₂O₂ only (Fig. S9), the peak was compared to one obtained for the same gold ion concentration (0.3M H_{AuCl₄}) with the addition of 200 μM H₂O₂ (i.e., 0.3M H_{AuCl₄} + 200 μM H₂O₂) and the new peak was found at the same position/chemical shift with relatively more intensity and no other additional peak/s was found in the spectra. This confirms that the peak at around 9.4 ppm corresponds to H₂O₂ only.

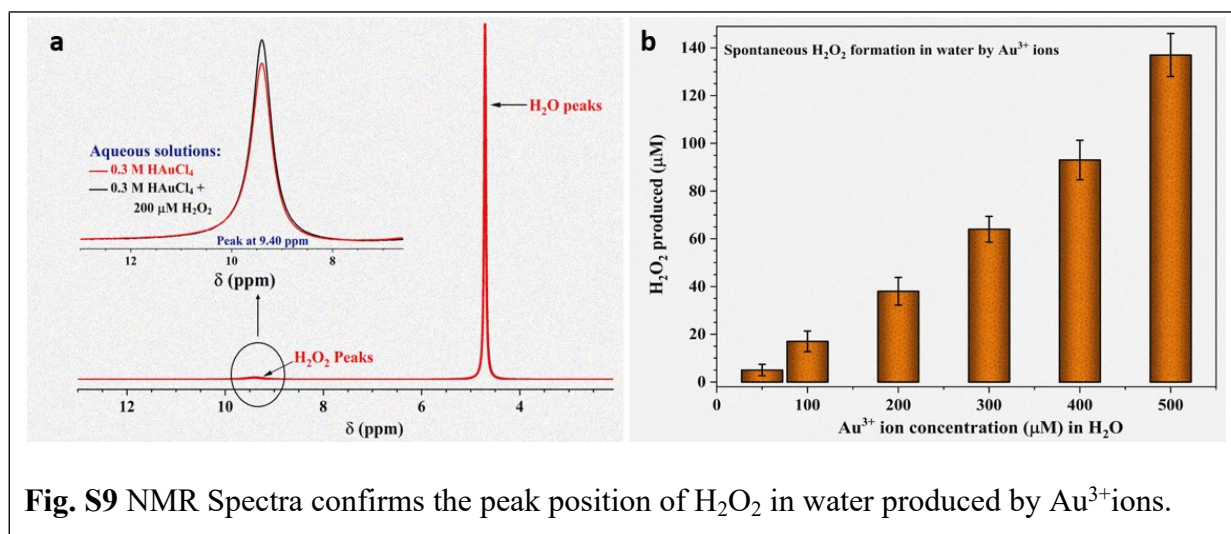
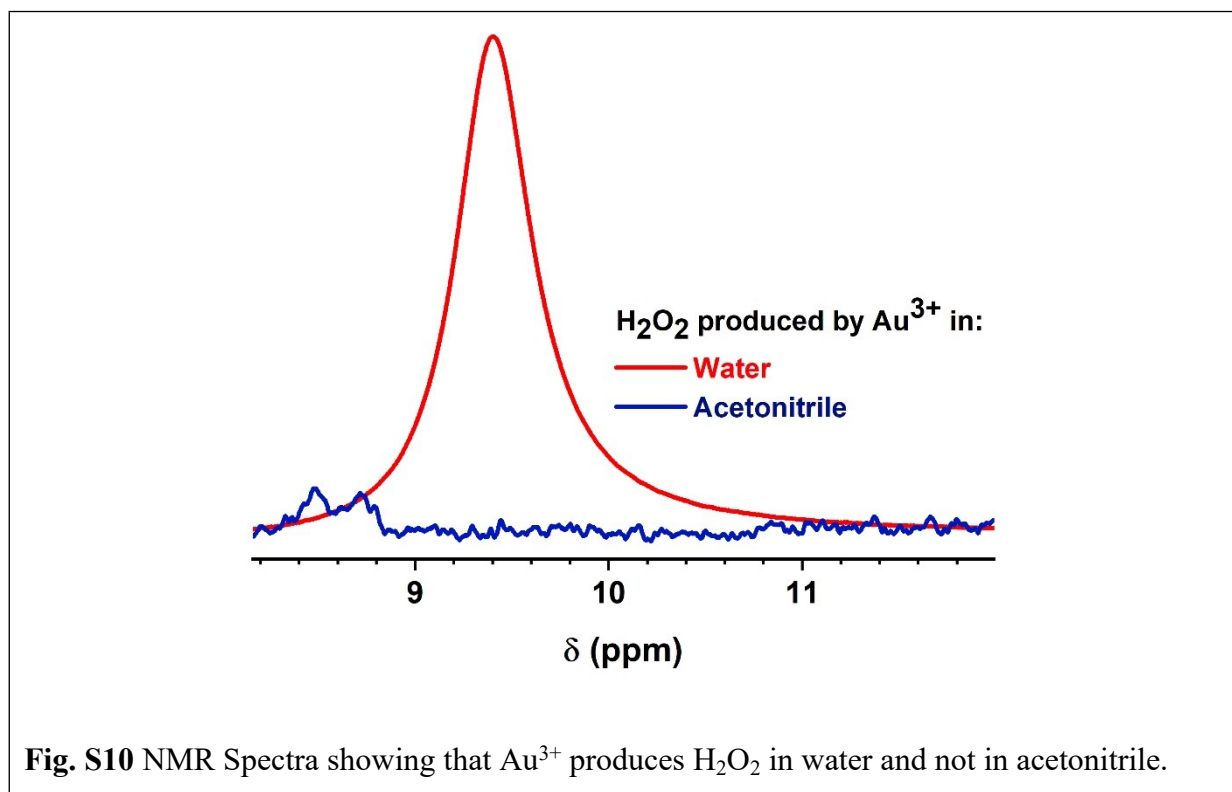


Fig. S9 NMR Spectra confirms the peak position of H₂O₂ in water produced by Au³⁺ ions.

Fig. S10 shows the data obtained for the same concentration of gold ion (Au^{3+}) in water and acetonitrile, which confirmed the formation of H_2O_2 in water and not in acetonitrile.



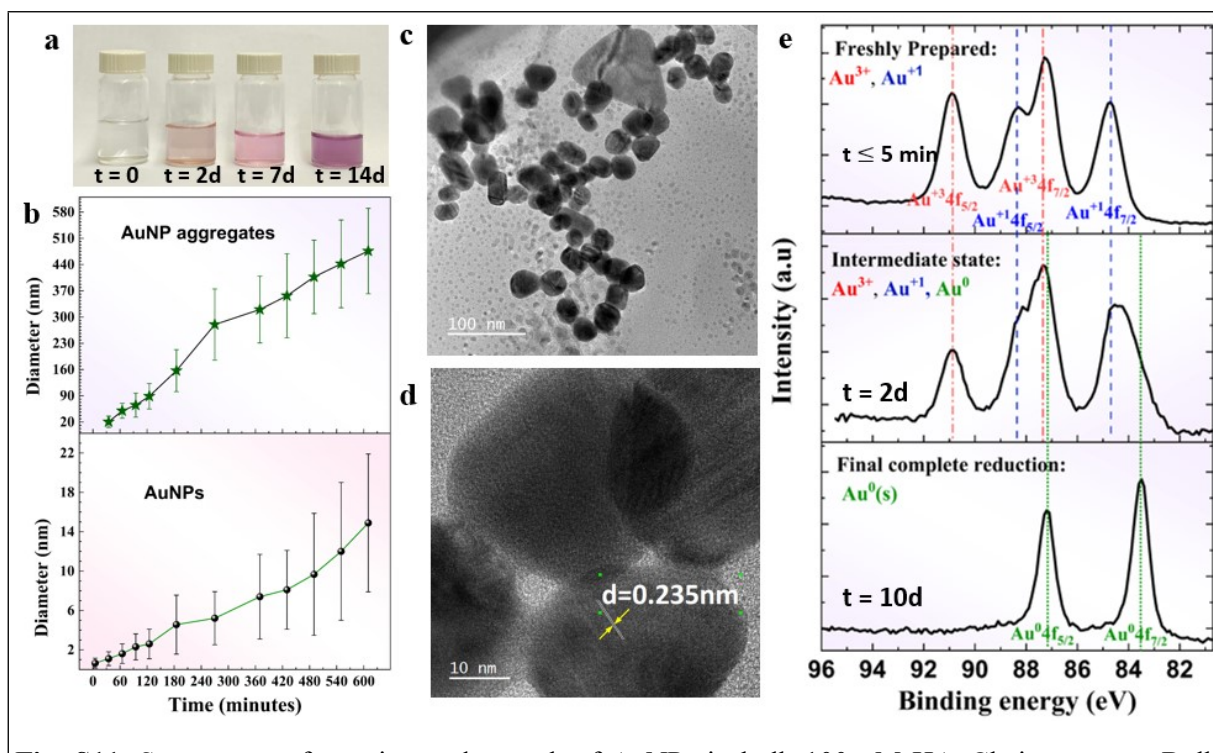


Fig. S11. Spontaneous formation and growth of AuNPs in bulk 100- μ M HAuCl_4 in water. **a** Bulk solution changing color due to the nucleation and growth of AuNPs. **b** Formation and growth of particles with time, as measured by DLS. **c** TEM micrograph showing the presence of AuNPs of different sizes. **d** TEM imaging showing an interlayer spacing of $\sim 0.235\text{ nm}$ corresponding to the Au(111) atomic plane of metallic gold $\text{Au}(0)$. **e** XPS analysis showing the presence of Au^{3+} and Au^{+} in freshly prepared solution, Au^{3+} , Au^{+} , and Au^0 in 2-day-old solution, and Au^0 in 10-days-old solution. Complete reduction of gold ions to AuNPs after some time.

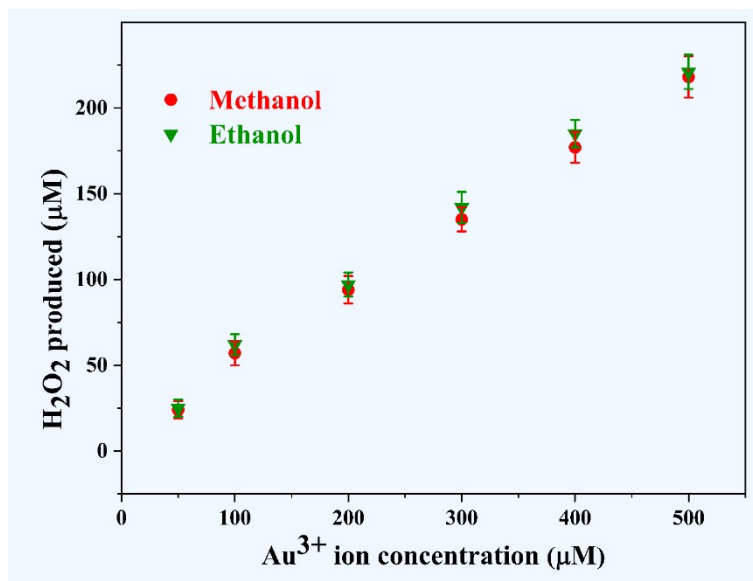


Fig. S12. Spontaneous formation of H₂O₂ by HAuCl₄ salt in methanol and ethanol. The results were obtained by the HPAK Assay kit. The results suggest that there is no significant difference in H₂O₂ formation by Au³⁺ ions in methanol and ethanol.

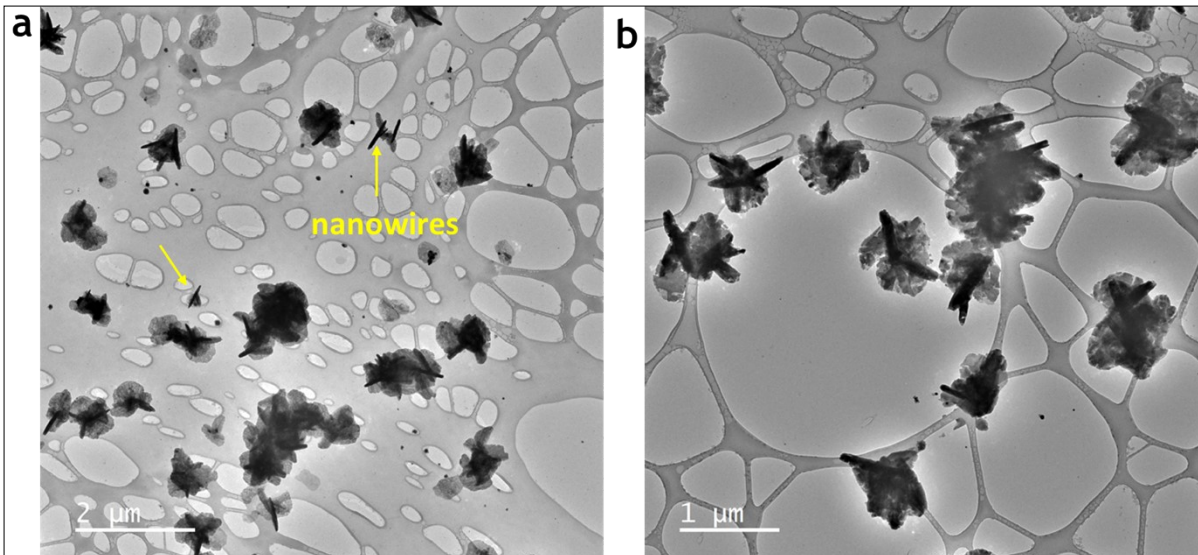


Fig. S13 TEM micrographs of bulk 200 μM HAuCl_4 aqueous solution. It clearly shows the presence of gold nanowires.

References:

1. Gallo Jr A, *et al.* On the formation of hydrogen peroxide in water microdroplets. *Chemical Science* **13**, 2574-2583 (2022).
2. Eatoo MA, Mishra H. Busting the myth of spontaneous formation of H₂O₂ at the air–water interface: contributions of the liquid–solid interface and dissolved oxygen exposed: *Chemical Science* **15**, 3093-3103 (2024).